

Machine Learning Potential Energy Surfaces

Oliver T. Unke and Markus Meuwly*

*Department of Chemistry, University of Basel, Klingelbergstrasse 80 , CH-4056 Basel,
Switzerland.*

E-mail: m.meuwly@unibas.ch

Machine Learning techniques can be used to represent high-dimensional potential energy surfaces for reactive chemical systems. Two such methods are based on a reproducing kernel Hilbert space representation or on deep neural networks. They can achieve a sub-1 kcal/mol accuracy with respect to reference data and can be used in studies of chemical dynamics. Their construction and a few typical examples are briefly summarized in the present contribution.

Abstract

1 Introduction

The potential energy surface (PES) - the way how atoms and molecules interact with one another - contains all information necessary to describe the structure and to follow the dynamics of molecular systems. Characterizing, interpreting and understanding the dynamics of homogeneous and heterogeneous systems at a molecular level is a formidable task.¹ Typical processes of interest are chemical reactions or functional motions in proteins. For chemical reactions the relevant process, i.e. bond breaking or bond formation, occurs on the femtosecond time scale whereas typical rates for solution phase reactions are in the range of

1 s^{-1} . In other words, during $\sim 10^{15}$ vibrational periods energy is redistributed in the system until sufficient energy has accumulated along the preferred “progression coordinate” for the reaction to occur. Another example, freezing and phase transitions in water are entirely governed by intermolecular interactions. Describing them at sufficient detail has been found extremely challenging and a complete understanding of the phase diagram or the structural dynamics of liquid water is still not available.²

Computing an experimentally observable quantity, such as a rate, infrared spectrum, or a diffusion coefficient, requires means to determine the total energy of the system accurately and efficiently. For MD simulations not only energies but also forces are required to propagate the equations of motion. One way is to solve the electronic Schrödinger equation for every configuration \vec{x} of the system. However, there are limitations which are due to the computational approach *per se*, e.g. the speed and efficiency of the method or due to practical aspects of quantum chemistry such as accounting for the basis set superposition error, the convergence of the Hartree-Fock wavefunction to the desired electronic state for arbitrary geometries, or the choice of a suitable active space irrespective of molecular geometry for problems with multi-reference character, to name a few. Improvements and future avenues for making QM-based approaches even more broadly applicable have been recently discussed.³ For problems that require extensive conformational sampling or sufficient statistics purely QM-based dynamics approaches are still impractical.

A promising use of QM-based methods are mixed quantum mechanics/molecular mechanics (QM/MM) treatments which are particularly popular for biophysical and biochemical applications.⁴ Here, the system is decomposed into a “reactive region” which is treated with a quantum chemical (or semiempirical) method and an environment described by an empirical force field. Such a decomposition considerably speeds up simulations such that even free energy simulations in multiple dimensions can be computed.⁵ One of the current open ques-

tions in such QM/MM simulations is that of the size of the QM region required for converged results which was recently considered for Catechol O-Methyltransferase.⁶

The most rigorous approach to reactive chemical dynamics is to use fully dimensional, reactive PESs, which are usually only available for low-dimensional systems. Specifically in the field of small molecule reactions involving processes such as $A+BC \rightarrow AB+C$ or $AB+CD \rightarrow A+BCD$ (or permutations thereof) involving a total number of 3 to 8 atoms the construction of globally valid potential energy surfaces is essential to make direct contact between computations and experiments. The limitation on up to 8 atoms is primarily owed to the fact that accurately solving the nuclear Schrödinger equation for systems involving a larger number of nuclei remains an unsolved problem although considerable progress has been made over the past several years.^{7,8}

One of the earliest efforts to determine outcomes of chemical reactions from dynamics studies is the $H+H_2$ atom exchange reaction. Using classical molecular dynamics (MD) and a modified London-Eyring-Polanyi-Sato (LEPS) surface,⁹⁻¹¹ the differential cross sections for the $D+H_2$ reaction were calculated.¹² Some 10 years later the results of these quasi-classical simulations were almost quantitatively confirmed at room temperature by a full quantum treatment.¹³

High-level *ab initio* calculations have become more accurate and more efficient.¹⁴⁻¹⁶ Along with the ever-increasing computational power it is now possible to compute thousands of energies at various geometries for small polyatomic systems within chemical accuracy (0.5 kcal/mol).¹⁷ With the availability of routine electronic structure calculations using large basis sets and accurate ways for approximately solving the electronic Schrödinger equation the problem shifted to *representing* the computed, discrete points on the PES. This is in particular needed when running MD simulations (classical or quasiclassical trajectory (QCT))

simulations) where the total energy and the derivatives at arbitrary points are required. Similarly, quantum wavepacket calculations require analytical forms of the PES whereas for collocation methods it is sometimes sufficient to work with a discrete, precomputed set of energies. Nevertheless, it is nowadays standard to represent nonreactive and reactive PESs in a manner that allows to evaluate it at arbitrary points, given pointwise information from *ab initio* calculations only. In addition, the final representation should be computationally efficient in order to run statistically significant numbers of (reactive) trajectories in QCT simulations.^{18–20}

A direct way for obtaining an analytical representation of a PES is to use a parametrized functional form^{21,22} and fit the parameters to a set of *ab initio* data using linear or non-linear least squares procedures.²³ For the specific case of van der Waals molecules such an approach has been very successful, in particular for applications in spectroscopy.^{21,24} Although such approaches have demonstrated to achieve root mean squared errors (RMSEs) within chemical accuracy,²⁵ choosing a functional form requires human intuition and the fitting itself can be tedious and time-intensive.^{26,27}

Over the past years alternative interpolation techniques including the modified Shepard interpolation,^{28–30} the moving least squares method,^{31–33} permutation invariant polynomials^{34–36} or neural network approaches^{37–39} have been used to obtain multi-dimensional reactive PESs.^{40–46} The total number of coefficients $D_{a_1 \dots a_m}$ grows rapidly with the number of atoms. For total polynomial order of 5 and 4 atoms (molecule ABCD with 4 different atoms) there are 462 such coefficients and for 5 atoms (molecule ABCDE) there are 3003 of them. Thus, the number of reference energies that need to be determined depends on the number of distinct coefficients for the fitting problem to be well-defined. Common to all these approaches is the fact that they primarily minimize the RMSE with respect to the training data. In this respect they are similar to parametrized fits..

2 Reproducing Kernel Hilbert Space (RKHS) PES

Machine-learning (ML) methods allow to estimate an unknown function value using a model that was “trained” with a set of known data.⁴⁷ For intermolecular interactions, Rabitz and coworkers^{48–50} have popularized the use of reproducing kernel Hilbert space (RKHS) theory⁵¹ that allows to construct a PES from a training set based on *ab initio* reference data. Such an approach is typically referred to as kernel ridge regression (KRR) in the ML community.^{47,52} The RKHS method has been successfully applied e.g. for constructing PESs for NO+O,²⁰ N₂⁺ + Ar⁵³ or H₂O.⁵⁴ A combination of expanding the PES in spherical harmonics for the angular coordinates and reproducing kernels for the radial coordinates has been explored for H₂⁺–He²⁶ and is now also used for larger systems.^{55,56}

To further automatize this process, dedicated computer code has been made available that generates the interpolation (and meaningful extrapolation) of the PES along with all required parameters automatically from gridded *ab initio* data.⁵⁷ The theory of reproducing kernel Hilbert spaces asserts that for given values $f_i = f(\mathbf{x}_i)$ of a function $f(\mathbf{x})$ for N training points \mathbf{x}_i , $f(\mathbf{x})$ can always be approximated as a linear combination of kernel products⁵⁸

$$\tilde{f}(\mathbf{x}) = \sum_{i=1}^N c_i K(\mathbf{x}, \mathbf{x}_i) \quad (1)$$

Here, the c_i are coefficients and $K(\mathbf{x}, \mathbf{x}')$ is the reproducing kernel of the RKHS. The coefficients c_i satisfy the linear relation

$$f_j = \sum_{i=1}^N c_i K_{ij} \quad (2)$$

with the symmetric, positive-definite kernel matrix $K_{ij} = K(\mathbf{x}_i, \mathbf{x}_j)$ and can therefore be calculated from the known values f_i in the training set by solving Eq. 2 for the unknowns

c_i using, e.g. Cholesky decomposition.⁵⁹ With the coefficients c_i determined, the function value at an arbitrary position \mathbf{x} can be calculated using Eq. 1. Derivatives of $\tilde{f}(\mathbf{x})$ of any order can be calculated analytically by replacing the kernel function $K(\mathbf{x}, \mathbf{x}')$ in Eq. 1 with its corresponding derivative.

For practical applications in chemical physics it is also of interest to mention that it is possible to handle incomplete grids with an RKHS interpolation.⁵⁰ This is important because even for triatomic systems it is possible that converging quantum chemical calculations turns out to be difficult for certain geometries. Under these circumstances the grid of target energies contains a “hole”.

The explicit form of the multi-dimensional kernel function $K(\mathbf{x}, \mathbf{x}')$ is chosen depending on the problem to be solved. In general, it is possible to construct D -dimensional kernels as tensor products of one-dimensional kernels $k(x, x')$

$$K(\mathbf{x}, \mathbf{x}') = \prod_{d=1}^D k^{(d)}(x^{(d)}, x'^{(d)}) \quad (3)$$

For the kernel functions $k(x, x')$ it is possible to encode physical knowledge, in particular about its long range behaviour. Explicit radial kernels include the reciprocal power decay kernel

$$k_{n,m}(x, x') = n^2 x_{>}^{-(m+1)} \text{B}(m+1, n) {}_2\text{F}_1 \left(-n+1, m+1; n+m+1; \frac{x_{<}}{x_{>}} \right) \quad (4)$$

or the exponential decay kernel

$$k_n(x, x') = \frac{n \cdot n!}{\beta^{2n-1}} e^{-\beta x_{>}} \sum_{k=0}^{n-1} \frac{(2n-2-k)!}{(n-1-k)!k!} [\beta(x_{>} - x_{<})]^k \quad (5)$$

where $x_{>}$ and $x_{<}$ are the larger and smaller of x and x' and the integer n determines the

smoothness. In Eq. 4 the parameter m is the long-range decay of the dominant intermolecular interaction (e.g. $m = 6$ for dispersion), $B(a, b)$ is the beta function and ${}_2F_1(a, b; c; d)$ is the Gauss hypergeometric function.

3 Deep Neural Networks

Artificial neural networks (NNs)^{60–66} are a popular class of ML algorithms to tackle computationally demanding problems.^{67,68} Specifically, NNs have been used previously to fit PESs for molecular systems in the spirit of many-body expansions.^{69–72} While being accurate, they typically involve a large number of individual NNs (one for each term in the many-body expansion), making the method scale poorly for large systems. An alternative approach, known as high-dimensional NN (HDNN) first applied to bulk silicon,^{73,74} decomposes the total energy of a system into atomic contributions, which is appealing, because “energy” is an extensive property and it allows to use the same network to systems of different size.

Deep tensor NN (DTNN)⁷⁵ are a conceptually different approach and allow to reuse the same NN to predict energies of systems with different composition across chemical space. Similar to HDNNs, DTNN accumulates atomic energy contributions to predict the total energy E_{tot} .

In an artificial neural network (ANN)^{60–66} neurons transform an input vector \mathbf{x} of dimension n to an output vector \mathbf{y} of dimension m through a transformation

$$\mathbf{y} = \mathbf{W}\mathbf{x} + \mathbf{b} \tag{6}$$

Here, \mathbf{W} is an $n \times m$ matrix containing weights and the biases \mathbf{b} are an n -vector whose both entries are parameters. A single dense layer NN can only represent linear relations between input and output. In order to model a non-linear relationship at least two dense layers are

required and combined with a non-linear activation function σ (e.g. a sigmoid function)

$$\mathbf{h} = \sigma(\mathbf{W}_1\mathbf{x} + \mathbf{b}_1) \quad (7)$$

$$\mathbf{y} = \mathbf{W}_2\mathbf{h} + \mathbf{b}_2 \quad (8)$$

Equations 7 and 8 are general function approximators with which any input \mathbf{x} can be mapped onto output \mathbf{y} to arbitrary precision, provided that the dimensionality of the “hidden layer” \mathbf{h} is large enough.^{76,77} As such, NNs are a natural choice for representing a PES, i.e. a mapping from chemical structure to energy. For an intermolecular PES the output \mathbf{y} is usually one-dimensional and represents the energy.

While *shallow* NNs with a single hidden layer are in principle sufficient to solve any learning task, in practice, *deep* NNs with multiple hidden layers are exponentially more parameter-efficient.⁷⁸ In a deep NN, l hidden layers are stacked on top of each other, which map the input \mathbf{x} to an increasingly complex feature space. In the final layer, the features \mathbf{h}_l are combined to the output \mathbf{y} . The parameters of the NN are initialized randomly and then optimized by minimization of a loss function which quantifies the difference between the output of the NN and the training data.

NN based on local descriptor: Using a strictly local chemical descriptor, a NN-based method tailored for accurate energy evaluations, which can be applied to construct PESs for nonre-active and reactive dynamics of chemically heterogeneous systems in the condensed phase, has been introduced.⁷⁹ For this, a descriptor has been built from representing the neighborhood density of an atom as a linear combination of a product of a radial Gaussian function and spherical harmonics. Training with 50000 structures from the QM9 data set yields an RMSE of 0.98 ± 0.04 kcal/mol compared with 1.37 ± 0.01 from DTNN.⁷⁵ The mean average errors are 0.46 ± 0.01 kcal/mol compared with 0.92 ± 0.01 kcal/mol from DTNN and

0.59 from SchNet.⁸⁰ Contrary to SchNet, this NN is more efficient because a local descriptor is used and the network architecture is much simpler. As forces can also be evaluated it is possible to train NN for reactive MD simulations. However, it should be noted that developing NN-based energy functions depends on the availability of extensive training data.

NN based on learnable descriptor: PhysNet, on the other hand, learns the atom descriptors during training. It combines reusable building blocks in a modular fashion to construct a DNN for predicting atomic contributions to properties (such as energy) of a chemical system composed of N atoms based on atomic features $\mathbf{x}_i \in \mathbb{R}^n$ (here, n denotes the dimensionality of the feature space). The features simultaneously encode information about nuclear charge Z and local atomic environment of each atom i and are constructed by iteratively refining an initial representation depending solely on Z_i through coupling with the feature vectors \mathbf{x}_j of all atoms $j \neq i$ within a cut-off radius r_{cut} . The *embedding layer* maps from a discrete object - atomic numbers - to a vector of real numbers. The *residual block* contains shortcut connection which help to maintain performance in learning as training proceeds. The *interaction block* uses atom positions in the features and is formulated in terms of pairwise distances which ensures translational and rotational invariance, and summation ensures permutational invariance. In this block, the interaction between a central atom i and its environment (atoms j within a cutoff distance) is iteratively refined based on attention masks that are biased towards $\exp(-r_{ij})$ to encode locality in bonded chemical interactions. Finally, the *output block* computes the result from each module by summation.

4 Applications

Dynamics studies of chemical reactions date back more than 50 years.¹² Since then the sophistication of the PESs and the accuracy with which the nuclear dynamics can be followed

have continuously increased.⁸¹ In the following a few examples for using RKHS- and NN-based reactive PESs are briefly discussed.

4.1 Small Molecule Reactions

Particularly interesting applications of reactive MD simulation concern physical conditions that are difficult to study in laboratory experiments, such as extremely high ($T \geq 10000$ K) temperatures as they occur in explosions or in hypersonics.⁸² As an example, the $\text{C}(^3\text{P}) + \text{NO}(\text{X}^2\Pi) \rightarrow \text{O}(^3\text{P}) + \text{CN}(\text{X}^2\Sigma^+)$, $\text{N}(^2\text{D})/\text{N}(^4\text{S}) + \text{CO}(\text{X}^1\Sigma^+)$ reactions of the [CNO] system are briefly considered.⁸³ Figure 1 shows the RKHS representations of the $^2\text{A}'$, $^2\text{A}''$ and $^4\text{A}''$ electronic states based on more than 50000 *ab initio* energies are calculated at the MRCI+Q/aug-cc-pVTZ level of theory. As can be appreciated some of the topographies of the PESs would be very demanding to be represented by a particular choice of a parametrized function, such as the $^2\text{A}''$ channel for N+CO. Under such circumstances an RKHS, data-driven ansatz is preferable.

These PESs can subsequently be used in quasi-classical or quantum studies. As an example, the rate for CN and CO formation from $\text{C}(^3\text{P}) + \text{NO}(\text{X}^2\Pi) \rightarrow \text{O}(^3\text{P}) + \text{CN}(\text{X}^2\Sigma^+)$ and $\text{N}(^2\text{D})/\text{N}(^4\text{S}) + \text{CO}(\text{X}^1\Sigma^+)$ is compared. Without inclusion of nonadiabatic effects the two experimentally determined rates are underestimated by $\sim 25\%$ whereas including them leads to quantitative agreement within error bars. As another finding it was shown that the product vibrational state distribution of CN and CO following the C+NO reaction from quasi-classical and quantum simulations are very similar for different collisional energies.

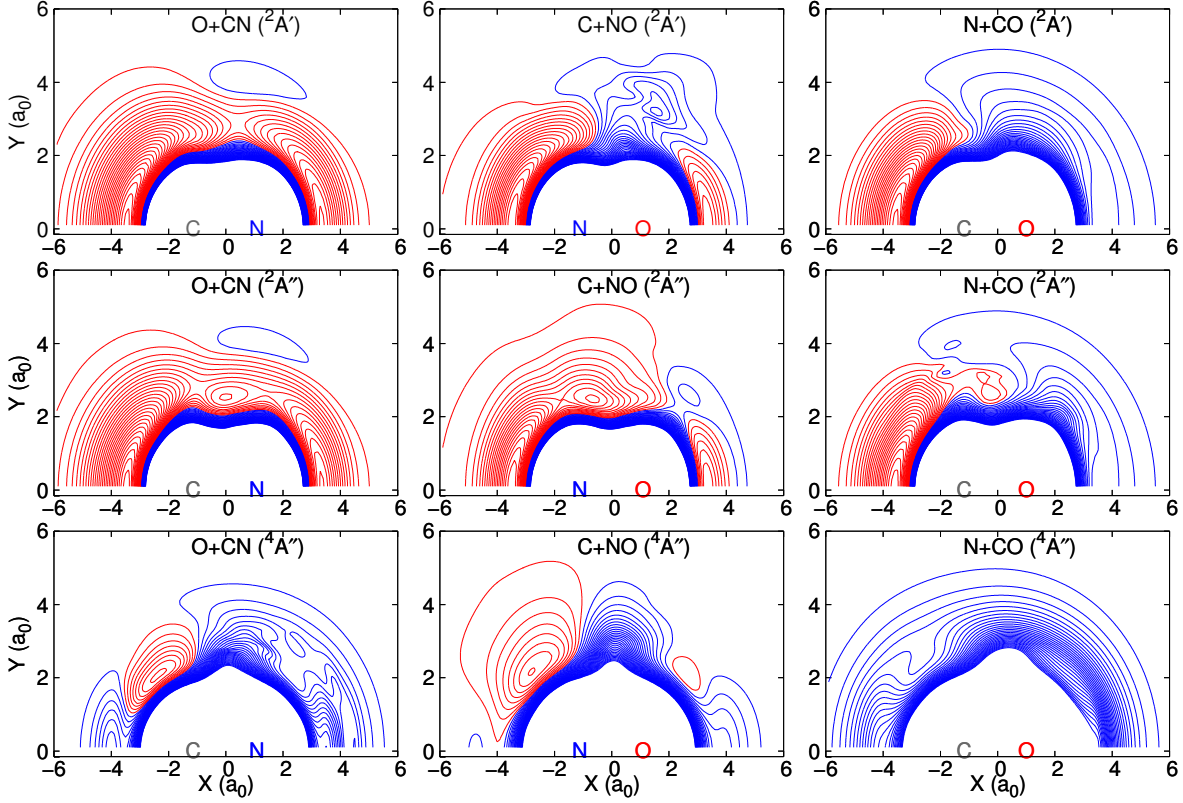


Figure 1: Contour plots of the analytical PESs with the diatoms having bond distances fixed at their equilibrium distances. Spacing between the contour lines is 0.2 eV. The red lines correspond to negative energies (-0.1, -0.3, -0.5, eV) and the blue lines correspond to positive energies (0.1, 0.3, 0.5, eV). Zero of energies set to the energy of the atoms and equilibrium configurations of the diatoms (*i. e.*, 2.234, 2.192 and 2.150 a_0 respectively for CN, NO and CO).

4.2 Reactive Dynamics using Neural Networks

Illustrative results for reactions are presented for a NN using the neighborhood representation for each atom for malonaldehyde⁷⁹ and for PhysNet trained on S_N2 reactions.⁸⁴ A reactive MD simulation was run using molecular mechanics with proton transfer⁸⁵ and the energies were evaluated at the MP2/6-311++G(d,p) level of theory and the NN trained on such energies. As is evident from figure 2, the quality of the NN is better than 0.5 kcal/mol which makes it competitive with an explicitly parametrized, reactive FF.

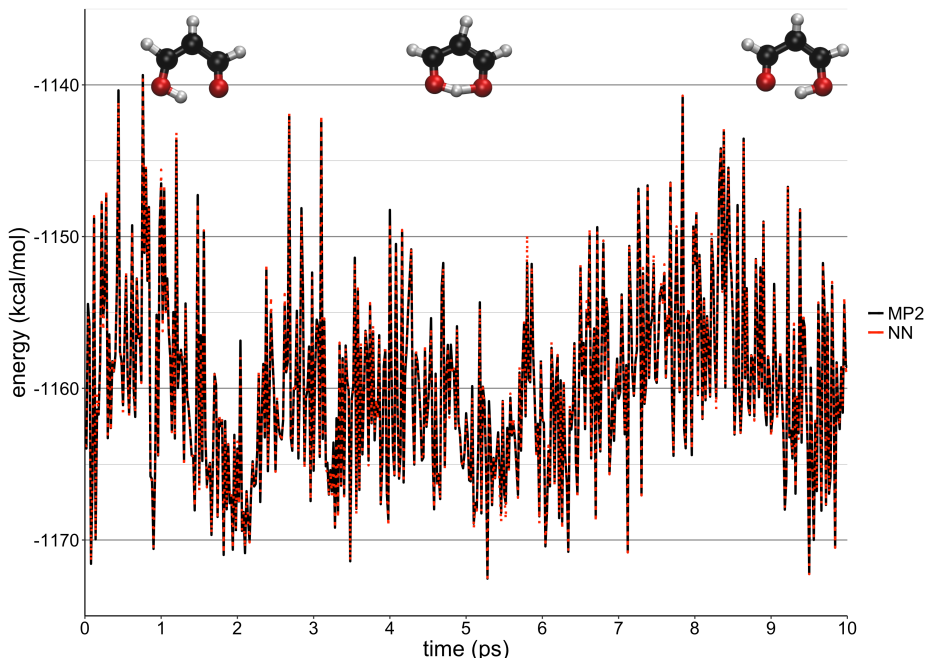


Figure 2: First 10 ps of a MD trajectory of malonaldehyde with intramolecular H-transfer. *Top panel:* Energy difference (absolute error) between MP2/6-311++G(d,p) reference energies and energies predicted by the NN trained on 100k reference structures. The error rarely exceeds 1 kcal mol⁻¹. *Bottom panel:* The solid black curve corresponds to the reference energies, the dotted red curve corresponds to the energies predicted by the NN. It is able to describe transition geometries and geometries close to equilibrium structures equally well.

Using PhysNet the reactive PESs for S_N2 reactions of the type XCH_3-Y (with X and Y being F, Cl, Br, and I) were learned. As reported in Figure 3 PhysNet without explicit long range already performs well, in particular for the minimum and transition state regions. However, including explicit long-range electrostatics further enhances the performance of

PhysNet which is also reflected in reducing the MAE from 0.070 kcal/mol to 0.009 kcal/mol.

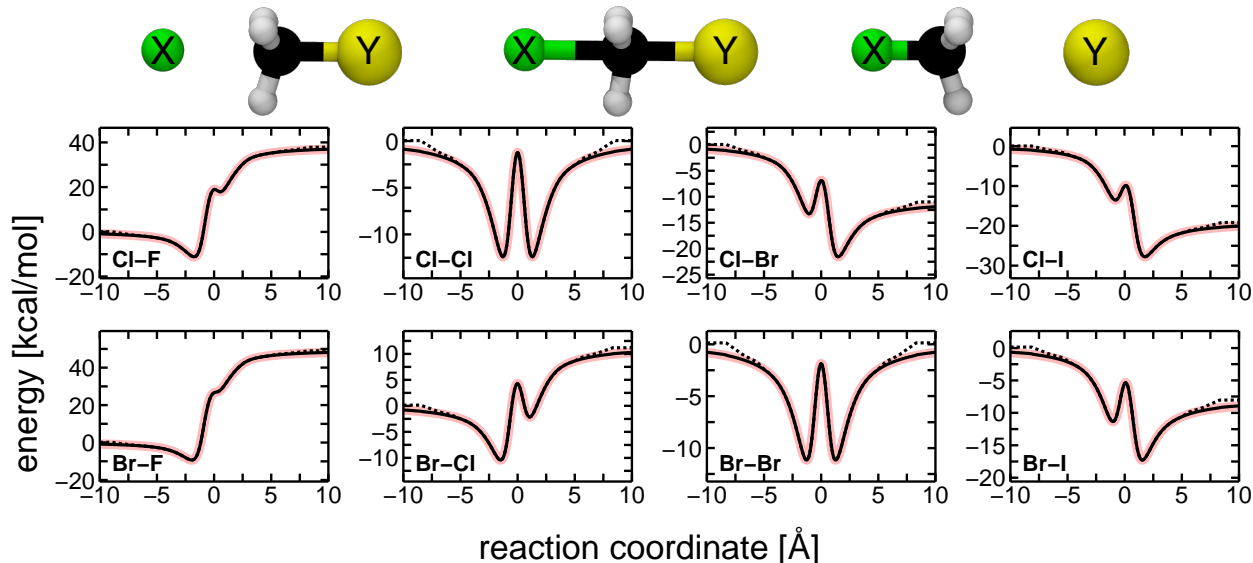


Figure 3: Minimum energy paths (MEPs) for S_N2 reactions $X^- + H_3C-Y \rightarrow X-CH_3 + Y^-$ along the reaction coordinate defined by the distance difference $r_{CY} - r_{CX}$, calculated using an ensemble of five NN models with (solid black line) and without (dotted black line) explicit long-range interactions. The light red envelope is the MEP calculated using the reference method. Each panel shows a different combination X-Y, as indicated. The NN including explicit long-range interactions is virtually identical to the reference method for all values of the reaction coordinate (apart from small deviations in the asymptotics), whereas the model without long-range interactions shows qualitatively wrong asymptotic behaviour for a comparison of prediction errors between both models).

5 Summary and Outlook

Methods based on machine learning provide a versatile and computationally robust and efficient framework to investigate the dynamics of molecular systems. The present contribution briefly discusses two avenues to generate high-accuracy representations based on electronic structure calculations. One of them uses an interpolation of gridded data based on reproducing kernels which is also capable of describing the correct long range behaviour of intermolecular interactions. The second approach (PhysNet) trains NNs to reference electronic structure data in order to run reactive MD simulations.

One of the challenges for RKHS-based methods is to extend them to higher-dimensional systems. Interesting work in this direction has recently been discussed in the framework of Gaussian Process learning which indicated that for accurate computation of differential cross sections of a typical diatom-diatom system ($\text{O}_2 + \text{OH}$) only 300 energies are required to specify the PES.⁸⁶ On the other hand, work based on permutationally invariant polynomials was able to parametrize a fully dimensional PES for N-methyl-acetamide.⁸⁷ Similar to a combination of RKHS-based and empirical FFs together with MS-ARMD to combine accurate representations of intermolecular interactions and the possibility to follow chemical reactions it may be possible to combine NN-based techniques with empirical FFs. Another future challenge concerns developing ML-learned representations for simulations in the condensed phase.

Acknowledgments

The authors acknowledge financial support from the Swiss National Science Foundation (NCCR-MUST and Grant No. 200021-7117810), the AFOSR, and the University of Basel.

References

- (1) El Hage, K.; Brickel, S.; Hermelin, S.; Gaulier, G.; Schmidt, C.; Bonacina, L.; van Keulen, S. C.; Bhattacharyya, S.; Chergui, M.; Hamm, P.; Rothlisberger, U.; Wolf, J.-P.; Meuwly, M. Implications of short time scale dynamics on long time processes. *Struct. Dyn.* **2017**, *4*.
- (2) Cisneros, G. A.; Wikfeldt, K. T.; Ojamae, L.; Lu, J.; Xu, Y.; Torabifard, H.; Bartok, A. P.; Csanyi, G.; Molinero, V.; Paesani, F. Modeling Molecular Interactions in Water: From Pairwise to Many Body Potential Energy Functions. *Chem. Rev.* **2016**, *116*, 7501–7528.

- (3) Cui, Q. Perspective: Quantum mechanical methods in biochemistry and biophysics. *J. Chem. Phys.* **2016**, *145*.
- (4) Senn, H. M.; Thiel, W. QM/MM Methods for Biomolecular Systems. *Angew. Chem. Intern. Ed.* **2009**, *48*, 1198–1229.
- (5) Roston, D.; Demapan, D.; Cui, Q. Leaving Group Ability Observably Affects Transition State Structure in a Single Enzyme Active Site. *J. Am. Chem. Soc.* **2016**, *138*, 7386–7394.
- (6) Kulik, H. J.; Zhang, J.; Klinman, J. P.; Martinez, T. J. How Large Should the QM Region Be in QM/MM Calculations? The Case of Catechol O-Methyltransferase. *J. Phys. Chem. B* **2016**, *120*, 11381–11394.
- (7) Zhang, W. et al. Depression of reactivity by the collision energy in the single barrier $\text{H} + \text{CD}_4 \rightarrow \text{HD} + \text{CD}_3$ reaction. *Proc. Natl. Acad. Sci.* **2010**, *107*, 12782–12785.
- (8) Zhao, Z.; Zhang, Z.; Liu, S.; Zhang, D. H. Dynamical barrier and isotope effects in the simplest substitution reaction via Walden inversion mechanism. *Nat. Comm.* **2017**, *8*.
- (9) Porter, R.; Karplus, M. Potential Energy Surface for H_3 . *J. Chem. Phys.* **1964**, *40*, 1105–1115.
- (10) Sato, S. On a new method of drawing the potential energy surface. *J. Chem. Phys.* **1955**, *23*, 592–593.
- (11) Sato, S. Potential energy surface of the system of three atoms. *J. Chem. Phys.* **1955**, *23*, 2465–2466.
- (12) Karplus, M.; Sharma, R.; Porter, R. Dynamics of reactive collisions: $\text{H} + \text{H}_2$ exchange reaction. *J. Chem. Phys.* **1964**, *40*, 2033–&.

- (13) Schatz, G.; Kuppermann, A. Quantum-Mechanical Scattering for 3-Dimensional Atom plus Diatom Systems: 2 Accurate Cross-Sections for $\text{H}+\text{H}_2$. *J. Chem. Phys.* **1976**, *65*, 4668–4692.
- (14) White, C. A.; Johnson, B. G.; Gill, P. M.; Head-Gordon, M. Linear Scaling Density Functional Calculations via the Continuous Fast Multipole Method. *Chem. Phys. Lett.* **1996**, *253*, 268–278.
- (15) Adler, T. B.; Knizia, G.; Werner, H.-J. A Simple and Efficient CCSD(T)-F12 Approximation. *J. Chem. Phys.* **2007**, *127*, 221106–224100.
- (16) Knizia, G.; Adler, T. B.; Werner, H.-J. Simplified CCSD(T)-F12 Methods: Theory and Benchmarks. *J. Chem. Phys.* **2009**, *130*, 054104.
- (17) Bokhan, D.; Ten-No, S.; Noga, J. Implementation of the CCSD(T)-F12 Method Using Cusp Conditions. *Phys. Chem. Chem. Phys.* **2008**, *10*, 3320–3326.
- (18) Yosa, J.; Meuwly, M. Vibrationally Induced Dissociation of Sulfuric Acid (H_2SO_4). *J. Phys. Chem. A* **2011**, *115*, 14350 – 14360.
- (19) Tong, X.; Nagy, T.; Reyes, J. Y.; Germann, M.; Meuwly, M.; Willitsch, S. State-selected ion-molecule reactions with Coulomb-crystallized molecular ions in traps. *Chem. Phys. Lett.* **2012**, *547*, 1–8.
- (20) Castro-Palacio, J. C.; Nagy, T.; Bemish, R. J.; Meuwly, M. Computational Study of Collisions Between $\text{O}(^3\text{P})$ and $\text{NO}(^2\Pi)$ at Temperatures Relevant to the Hypersonic Flight Regime. *J. Chem. Phys.* **2014**, *141*, 164319.
- (21) Hutson, J. Intermolecular forces from the spectroscopy of vanderwaals molecules. *Ann. Rev. Phys. Chem.* **1990**, *41*, 123–154.
- (22) Aguado, A.; Paniagua, M. A New Functional Form to Obtain Analytical Potentials of Triatomic Molecules. *J. Chem. Phys.* **1992**, *96*, 1265–1275.

- (23) Law, M. M.; Hutson, J. M. I-NoLLS: A Program for Interactive Nonlinear Least-Squares Fitting of the Parameters of Physical Models. *Comput. Phys. Commun.* **1997**, *102*, 252–268.
- (24) Roche, C.; Ernesti, A.; Hutson, J.; Dickinson, A. Evaluation of existing potential energy surfaces for CO₂-Ar: Pressure broadening and high-resolution spectroscopy of van der Waals complexes. *J. Chem. Phys.* **1996**, *104*, 2156–2166.
- (25) Boothroyd, A. I.; Keogh, W. J.; Martin, P. G.; Peterson, M. R. A Refined H₃ Potential Energy Surface. *J. Chem. Phys.* **1996**, *104*, 7139–7152.
- (26) Meuwly, M.; Hutson, J. The potential energy surface and near-dissociation states of He-H-2(+). *J. Chem. Phys.* **1999**, *110*, 3418–3427.
- (27) Mas, E.; Bukowski, R.; Szalewicz, K.; Groenenboom, G.; Wormer, P.; van der Avoird, A. Water pair potential of near spectroscopic accuracy. I. Analysis of potential surface and virial coefficients. *J. Chem. Phys.* **2000**, *113*, 6687–6701.
- (28) Franke, R.; Nielson, G. Smooth Interpolation of Large Sets of Scattered Data. *Int. J. Numer. Meth. Eng.* **1980**, *15*, 1691–1704.
- (29) Nguyen, K. A.; Rossi, I.; Truhlar, D. G. A Dual-Level Shepard Interpolation Method for Generating Potential Energy Surfaces for Dynamics Calculations. *J. Chem. Phys.* **1995**, *103*, 5522–5530.
- (30) Bettens, R. P.; Collins, M. A. Learning to Interpolate Molecular Potential Energy Surfaces with Confidence: A Bayesian Approach. *J. Chem. Phys.* **1999**, *111*, 816–826.
- (31) Lancaster, P.; Salkauskas, K. Surfaces Generated by Moving Least Squares Methods. *Math. Comp.* **1981**, *37*, 141–158.
- (32) Ischtwan, J.; Collins, M. A. Molecular Potential Energy Surfaces by Interpolation. *J. Chem. Phys.* **1994**, *100*, 8080–8088.

- (33) Dawes, R.; Thompson, D. L.; Wagner, A. F.; Minkoff, M. Interpolating Moving Least-Squares Methods for Fitting Potential Energy Surfaces: A Strategy for Efficient Automatic Data Point Placement in High Dimensions. *J. Chem. Phys.* **2008**, *128*, 084107.
- (34) Cassam-Chenaï, P.; Patras, F. Symmetry-Adapted Polynomial Basis for Global Potential Energy Surfaces-Applications to XY_4 Molecules. *J. Math. Chem.* **2008**, *44*, 938–966.
- (35) Braams, B. J.; Bowman, J. M. Permutationally Invariant Potential Energy Surfaces in High Dimensionality. *Int. Rev. Phys. Chem.* **2009**, *28*, 577–606.
- (36) Paukku, Y.; Yang, K. R.; Varga, Z.; Truhlar, D. G. Global Ab Initio Ground-State Potential Energy Surface of N_4 . *J. Chem. Phys.* **2013**, *139*, 044309.
- (37) Sumpter, B. G.; Noid, D. W. Potential Energy Surfaces for Macromolecules. A Neural Network Technique. *Chem. Phys. Lett.* **1992**, *192*, 455–462.
- (38) Bowman, J. M.; Braams, B. J.; Carter, S.; Chen, C.; Czako, G.; Fu, B.; Huang, X.; Kamarchik, E.; Sharma, A. R.; Shepler, B. C.; *et al.*, Ab-Initio-Based Potential Energy Surfaces for Complex Molecules and Molecular Complexes. *J. Phys. Chem. Lett.* **2010**, *1*, 1866–1874.
- (39) Jiang, B.; Li, J.; Guo, H. Potential Energy Surfaces from High Fidelity Fitting of Ab Initio Points: the Permutation Invariant Polynomial-Neural Network Approach. *Int. Rev. Phys. Chem.* **2016**, *35*, 479–506.
- (40) Jordan, M. J.; Thompson, K. C.; Collins, M. A. The Utility of Higher Order Derivatives in Constructing Molecular Potential Energy Surfaces by Interpolation. *J. Chem. Phys.* **1995**, *103*, 9669–9675.
- (41) Jordan, M. J.; Thompson, K. C.; Collins, M. A. Convergence of Molecular Potential

- Energy Surfaces by Interpolation: Application to the $\text{OH} + \text{H}_2 \rightarrow \text{H}_2\text{O} + \text{H}$ Reaction. *J. Chem. Phys.* **1995**, *102*, 5647–5657.
- (42) Skokov, S.; Peterson, K. A.; Bowman, J. M. An Accurate Ab Initio HOCl Potential Energy Surface, Vibrational and Rotational Calculations, and Comparison with Experiment. *J. Chem. Phys.* **1998**, *109*, 2662–2671.
- (43) Collins, M. A. Molecular Potential-Energy Surfaces for Chemical Reaction Dynamics. *Theor. Chem. Acc.* **2002**, *108*, 313–324.
- (44) Duchovic, R. J.; Volobuev, Y. L.; Lynch, G. C.; Truhlar, D. G.; Allison, T. C.; Wagner, A. F.; Garrett, B. C.; Corchado, J. C. POTLIB 2001: A Potential Energy Surface Library for Chemical Systems. *Comput. Phys. Commun.* **2002**, *144*, 169–187.
- (45) Zhang, X.; Braams, B. J.; Bowman, J. M. An Ab Initio Potential Surface Describing Abstraction and Exchange for $\text{H} + \text{CH}_4$. *J. Chem. Phys.* **2006**, *124*, 021104.
- (46) Li, J.; Wang, Y.; Jiang, B.; Ma, J.; Dawes, R.; Xie, D.; Bowman, J. M.; Guo, H. Communication: A Chemically Accurate Global Potential Energy Surface for the $\text{HO} + \text{CO} \rightarrow \text{H} + \text{CO}_2$ Reaction. *J. Chem. Phys.* **2012**, *136*, 041103.
- (47) Rupp, M. Machine Learning for Quantum Mechanics in a Nutshell. *Int. J. Quantum Chem.* **2015**, *115*, 1058–1073.
- (48) Ho, T.-S.; Rabitz, H. A General Method for Constructing Multidimensional Molecular Potential Energy Surfaces from Ab Initio Calculations. *J. Chem. Phys.* **1996**, *104*, 2584–2597.
- (49) Hollebeek, T.; Ho, T.-S.; Rabitz, H. A Fast Algorithm for Evaluating Multidimensional Potential Energy Surfaces. *J. Chem. Phys.* **1997**, *106*, 7223–7227.
- (50) Hollebeek, T.; Ho, T.-S.; Rabitz, H. Constructing Multidimensional Molecular Potential Energy Surfaces from Ab Initio Data. *Annu. Rev. Phys. Chem.* **1999**, *50*, 537–570.

- (51) Aronszajn, N. Theory of Reproducing Kernels. *Trans. Amer. Math. Soc.* **1950**, *68*, 337–404.
- (52) Hofmann, T.; Schölkopf, B.; Smola, A. J. Kernel methods in machine learning. *Ann. Stat.* **2008**, 1171–1220.
- (53) Unke, O. T.; Castro-Palacio, J. C.; Bemish, R. J.; Meuwly, M. Collision-Induced Rotational Excitation in N^{2+} ($^2\Sigma_g^+$, $\nu = 0$)–Ar: Comparison of Computations and Experiment. *J. Chem. Phys.* **2016**, *144*, 224307.
- (54) Ho, T.-S.; Hollebeek, T.; Rabitz, H.; Harding, L. B.; Schatz, G. C. A Global H_2O Potential Energy Surface for the Reaction $\text{O}(^1\text{D}) + \text{H}_2 \rightarrow \text{OH} + \text{H}$. *J. Chem. Phys.* **1996**, *105*, 10472–10486.
- (55) Dhont, G.; van Lenthe, J.; Groenenboom, G.; van der Avoird, A. Ab initio calculation of the $\text{NH}(^3\Sigma^-)$ - $\text{NH}(^3\Sigma^-)$ interaction potentials in the quintet, triplet, and singlet states. *J. Chem. Phys.* **2005**, *123*.
- (56) van der Avoird, A.; Pedersen, T. B.; Dhont, G. S. F.; Fernandez, B.; Koch, H. Ab initio potential-energy surface and rovibrational states of the HCN-HCl complex. *J. Chem. Phys.* **2006**, *124*.
- (57) Unke, O. T.; Meuwly, M. Toolkit for the Construction of Reproducing Kernel-Based Representations of Data: Application to Multidimensional Potential Energy Surfaces. *J. Chem. Inf. Model.* **2017**, *57*, 1923–1931.
- (58) Schölkopf, B.; Herbrich, R.; Smola, A. J. A Generalized Representer Theorem. International Conference on Computational Learning Theory. 2001; pp 416–426.
- (59) Golub, G. H.; Van Loan, C. F. *Matrix Computations*; JHU Press Baltimore, 2012; Vol. 3.

- (60) McCulloch, W. S.; Pitts, W. A Logical Calculus of the Ideas Immanent in Nervous Activity. *Bull. Math. Biophys.* **1943**, *5*, 115–133.
- (61) Kohonen, T. An Introduction to Neural Computing. *Neural Netw.* **1988**, *1*, 3–16.
- (62) Abdi, H. A Neural Network Primer. *J. Biol. Syst.* **1994**, *2*, 247–281.
- (63) Bishop, C. M. *Neural Networks for Pattern Recognition*; Oxford university press, 1995.
- (64) Clark, J. W. *Scientific Applications of Neural Nets*; Springer, 1999; pp 1–96.
- (65) Ripley, B. D. *Pattern Recognition and Neural Networks*; Cambridge university press, 2007.
- (66) Haykin, S. S. *Neural Networks and Learning Machines*; Pearson Upper Saddle River, NJ, USA.; 2009; Vol. 3.
- (67) Hinton, G.; Deng, L.; Yu, D.; Dahl, G. E.; Mohamed, A.-R.; Jaitly, N.; Senior, A.; Vanhoucke, V.; Nguyen, P.; Sainath, T. N. Deep Neural Networks for Acoustic Modeling in Speech Recognition: The Shared Views of Four Research Groups. *IEEE Signal Process. Mag.* **2012**, *29*, 82–97.
- (68) Lawrence, S.; Giles, C. L.; Tsoi, A. C.; Back, A. D. Face Recognition: A Convolutional Neural-Network Approach. *IEEE Trans. Neural Netw.* **1997**, *8*, 98–113.
- (69) Manzhos, S.; Carrington Jr, T. A Random-Sampling High Dimensional Model Representation Neural Network for Building Potential Energy Surfaces. *J. Chem. Phys.* **2006**, *125*, 084109.
- (70) Manzhos, S.; Carrington Jr, T. Using Redundant Coordinates to Represent Potential Energy Surfaces with Lower-Dimensional Functions. *J. Chem. Phys.* **2007**, *127*, 014103.
- (71) Malshe, M.; Narulkar, R.; Raff, L.; Hagan, M.; Bukkapatnam, S.; Agrawal, P.; Komanduri, R. Development of Generalized Potential-Energy Surfaces using Many-Body

- Expansions, Neural Networks, and Moiety Energy Approximations. *J. Chem. Phys.* **2009**, *130*, 184102.
- (72) Handley, C. M.; Popelier, P. L. Potential Energy Surfaces Fitted by Artificial Neural Networks. *J. Phys. Chem. A* **2010**, *114*, 3371–3383.
- (73) Behler, J.; Parrinello, M. Generalized Neural-Network Representation of High-Dimensional Potential-Energy Surfaces. *Phys. Rev. Lett.* **2007**, *98*, 146401.
- (74) Behler, J. Neural Network Potential-Energy Surfaces in Chemistry: A Tool for Large-Scale Simulations. *Phys. Chem. Chem. Phys.* **2011**, *13*, 17930–17955.
- (75) Schütt, K. T.; Arbabzadah, F.; Chmiela, S.; Müller, K. R.; Tkatchenko, A. Quantum-Chemical Insights from Deep Tensor Neural Networks. *Nat. Commun.* **2017**, *8*, 13890.
- (76) Cybenko, G. Approximation by superposition of sigmoidal functions. *Math. Control Signals Syst.* **1989**, *2*, 303–314.
- (77) Hornik, K. Approximation Capabilities of Multilayer Feedforward Networks. *Neural Netw.* **1991**, *4*, 251–257.
- (78) Eldan, R.; Shamir, O. The Power of Depth for Feedforward Neural Networks. Conference on Learning Theory. 2016; pp 907–940.
- (79) Unke, O. T.; Muwly, M. A Reactive, Scalable and Transferable Model for Molecular Energies from a Neural Network Approach Based on Local Information. *J. Chem. Phys.* **2018**, *148*, 241708.
- (80) Schütt, K. T.; Kindermans, P.; Sauceda, H.; Chmiela, S.; Tkatchenko, A.; Müller, K. SchNet: A Continuous-Filter Convolutional Neural Network for Modeling Quantum Interactions. 2017.
- (81) Bowman, J. M.; Czako, G.; Fu, B. High-dimensional ab initio potential energy surfaces for reaction dynamics calculations. *Phys. Chem. Chem. Phys.* **2011**, *13*, 8094–8111.

- (82) Millikan, R. C.; White, D. R. Systematics of vibrational relaxation. *J. Chem. Phys.* **1963**, *39*, 3209.
- (83) Koner, D.; Bemish, R. J.; Meuwly, M. The C(P-3) + NO(X-2 Pi) -> O(P-3) + CN(X-2 Sigma(+)), N(D-2)/N(S-4) + CO(X-1 Sigma(+)) reaction: Rates, branching ratios, and final states from 15 K to 20 000 K. *J. Chem. Phys.* **2018**, *149*.
- (84) Unke, O. T.; Meuwly, M. PhysNet: a neural network for predicting energies, forces, dipole moments and partial charges. *J. Chem. Theo. Comp.* **2019**,
- (85) Lammers, S.; Lutz, S.; Meuwly, M. Reactive force fields for proton transfer dynamics. *J. Comput. Chem.* **2008**, *29*, 1048–1063.
- (86) Vargas-Hernandez, R. A.; Guan, Y.; Zhang, D. H.; Krems, R., V Bayesian optimization for the inverse scattering problem in quantum reaction dynamics. **2019**, *21*.
- (87) Qu, C.; Bowman, J. M. A fragmented, permutationally invariant polynomial approach for potential energy surfaces of large molecules: Application to N-methyl acetamide. *J. Chem. Phys.* **2019**, *150*.